Supporting Information for

Probing electrochemical reactivity in an Sb_2S_3-containing potassium-ion battery anode: observation of an increased capacity

V. Lakshmi[a], Alexey A. Mikhaylov[b], Alexander G. Medvedev[b], Chao Zhang[c,d], Thrinathreddy Ramireddy[e,f], Md Mokhlesur Rahman[a], Pavel Cizek[a], Dmitri Golberg[c,d,g], Ying Chen[a], Ovadia Lev[h], Petr V. Prikhodchenko[b,*], Alexey M. Glushenkov[e,f,*]

[a] *Institute for Frontier Materials, Deakin University, Geelong Campus at Waurn Ponds, VIC 3216, Australia*

[b] *Kurnakov Institute of General and Inorganic Chemistry, Russian Academy of Sciences, Leninskii prosp. 31, Moscow 119991, Russian Federation*

[c] *Centre for Materials Science, Queensland University of Technology (QUT), 2nd George str., Brisbane, QLD 4000, Australia*

[d] *School of Chemistry and Physics, Queensland University of Technology (QUT), 2nd George str., Brisbane, QLD 4000, Australia*

[e] *Research School of Chemistry, The Australian National University, Canberra, ACT 2601, Australia*

[f] *Research School of Electrical, Energy and Materials Engineering, The Australian National University, Canberra, ACT 2601, Australia*

[g] *International Centre for Materials Nanoarchitectonics (MANA), National Institute for Materials Science (NIMS), Namik 1-1, Tsukuba, Ibaraki 3050044, Japan*

[h] *The Casali Center of Applied Chemistry, The Institute of Chemistry, The Hebrew University of Jerusalem, Edmond J. Safra Campus, Jerusalem 91904, Israel*

* Corresponding authors. Email: prikhman@gmail.com; alexey.glushenkov@anu.edu.au

Part 1. Additional electron microscopy characterisation data.

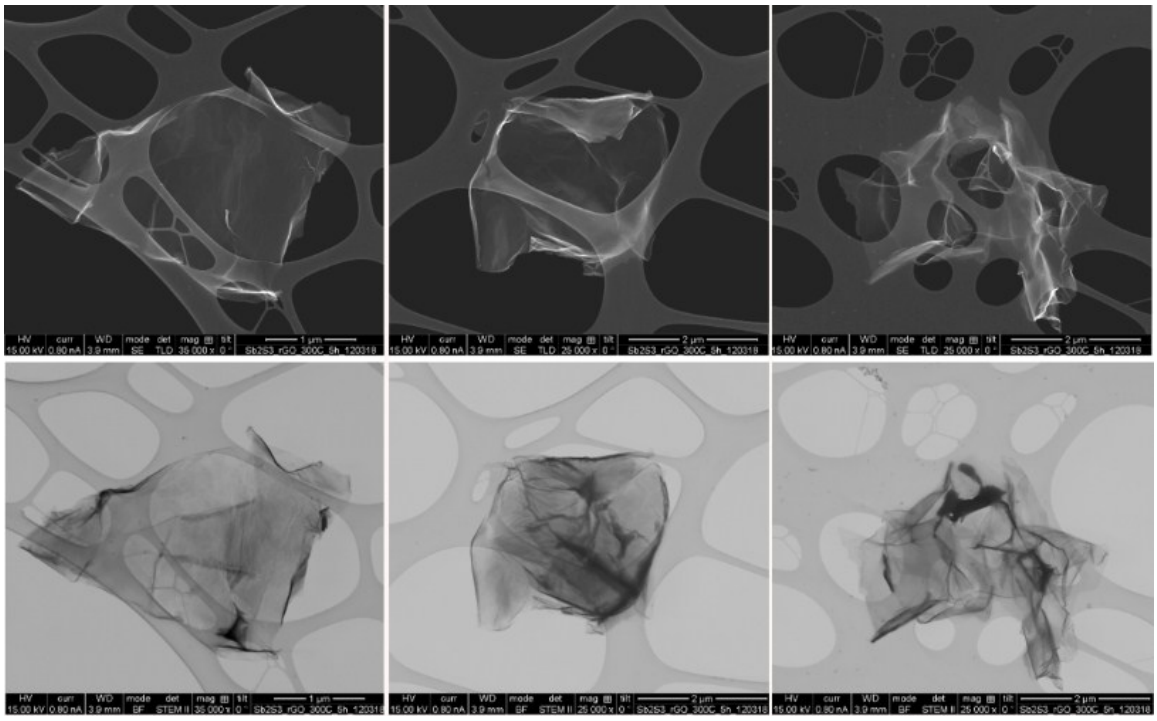

Fig. S1. Additional SEM and bright-field STEM images acquired from three locations: top row – SEM images; bottom row – STEM images simultaneously acquired from the same locations.

Part 2. Electrochemical performance of a commercial Sb_2S_3 powder

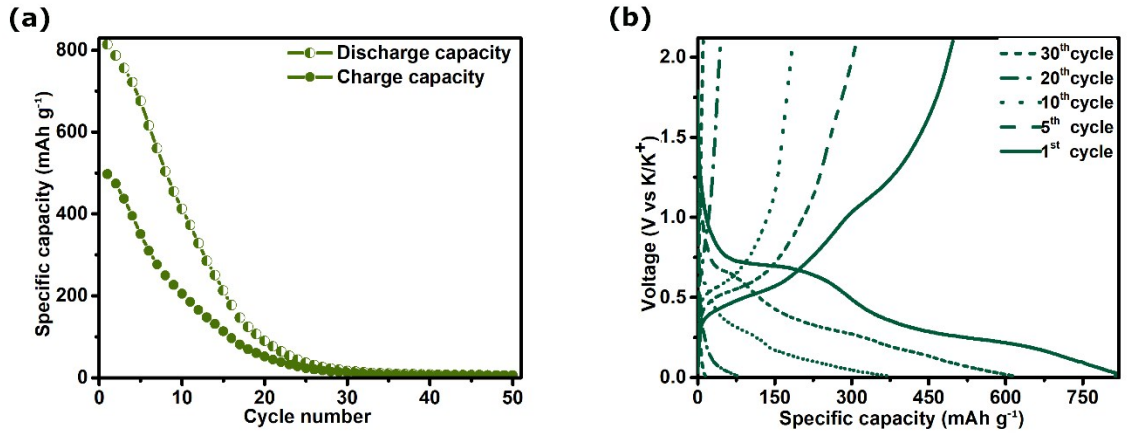

Fig. S2. The plot of charge and discharge capacities vs cycle number (a) and selected charge-discharge profiles at a current rate of 50 mA g^{-1} (b) for an electrode prepared with a commercial Sb_2S_3 powder.

Part 3. Cyclic voltammetry of Sb_2S_3-rGO

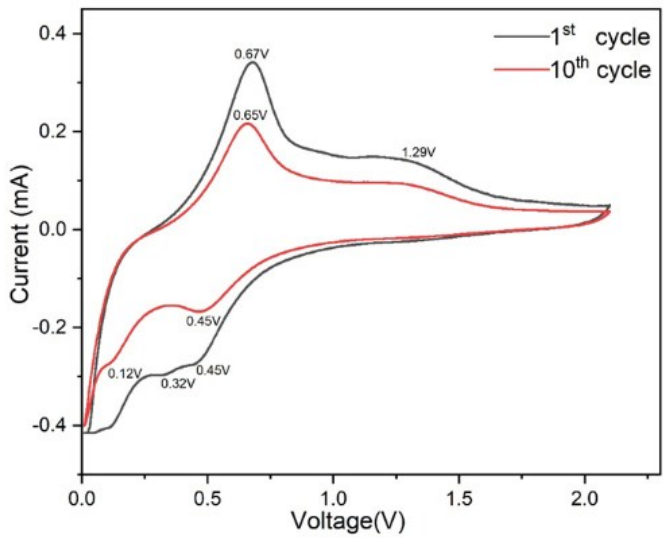

Fig. S3. Cyclic voltammetry curves of the Sb_2S_3-rGO composite in the first and tenth cycles at a sweep rate of 0.25 mV s^{-1}.

Part 4. Charge-discharge curves of Sb_2S_3-rGO in EC/DEC-based electrolyte

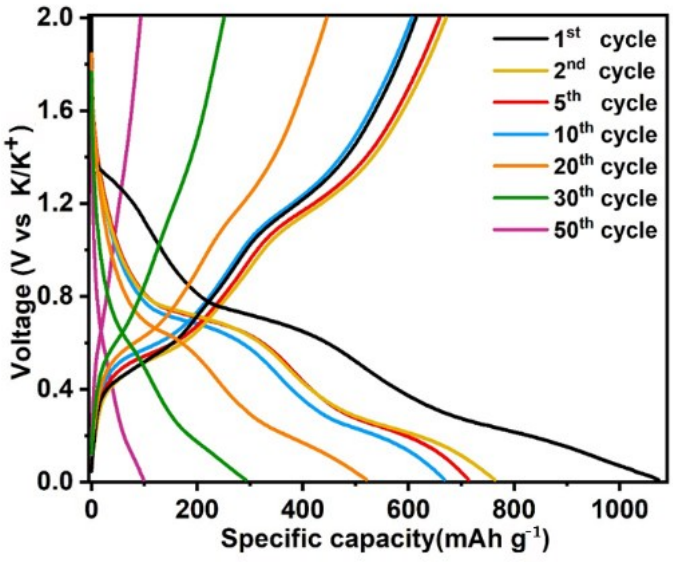

Fig. S4. Selected charge-discharge profiles for the Sb_2S_3-rGO composite in 1M KPF_6 in EC/DEC electrolyte at a current rate of 50 mA g^{-1}.

Part 5. Charge-discharge curves of Sb_2S_3-rGO in DME-based electrolyte

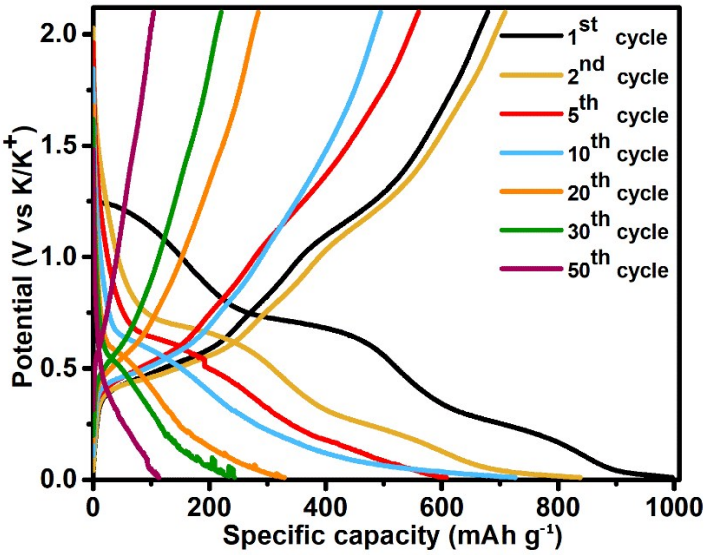

Fig. S5. Selected charge-discharge profiles for the Sb_2S_3-rGO composite in 1M KPF_6 in DME electrolyte at a current rate of 50 mA g^{-1}.

Part 6. Charge-discharge profiles for cycling in two potential ranges

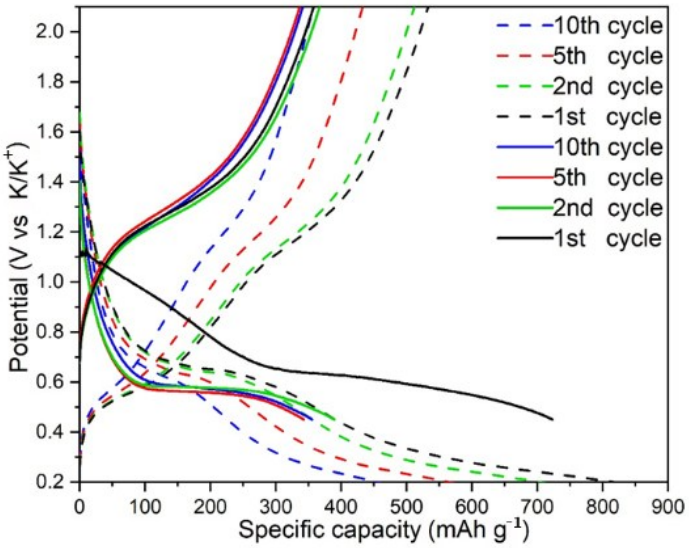

Fig. S6. Selected charge-discharge profiles obtained for the Sb_2S_3-rGO electrodes in two potential ranges (solid lines: 0.45-2.1 V vs K/K^+ and dotted lines: 0.18-2.1 V vs K/K^+).

Part 7. Coulombic efficiencies in different potential ranges

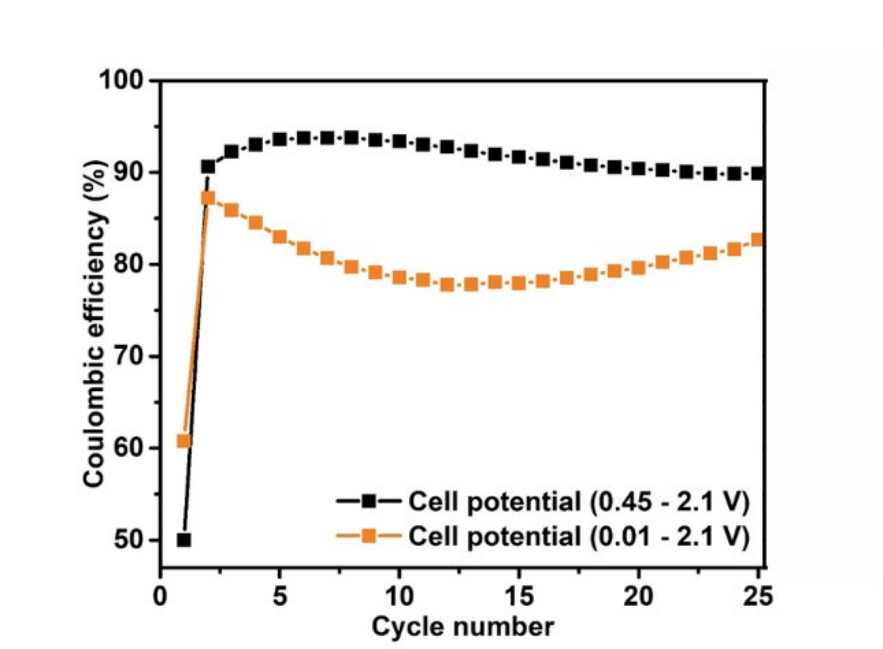

Fig. S7. Coulombic efficiencies observed in the initial cycles for Sb_2S_3-rGO electrodes in potential ranges 0.01 – 2.1 V vs K/K^+ and 0.45 – 2.1 V vs K/K^+.

Part 8. Data (recorded imaged and electron diffraction patterns in .dm4 format) for in-situ TEM experiments

Files have been uploaded separately as .zip archives. Archive names are

in_situ_TEM_location1.zip and **in_situ_TEM_location2.zip**

Each .dm4 frame contains acquisition time as a part of file name.